Article

Not peer-reviewed version

Cationic Azobenzenes as Light-Responsive Crosslinkers for Alginate-Based Supramolecular Hydrogels

Miriam Di Martino , Lucia Sessa * , Barbara Panunzi , Rosita Diana , Stefano Piotto , Simona Concilio *

Posted Date: 8 March 2024

doi: 10.20944/preprints202403.0536.v1

Keywords: Ionic Azobenzenes; Photoisomerization; Supramolecular hydrogels; Sodium alginate; Crosslinkers

 doi:10.20944/preprints202403.0536.v1

Article

Cationic Azobenzenes as Light-Responsive Crosslinkers for Alginate-Based Supramolecular Hydrogels

Miriam Di Martino [1], Lucia Sessa [1,*], Barbara Panunzi [2], Rosita Diana [2], Stefano Piotto [1,3] and Simona Concilio [1,3,*]

[1] Department of Pharmacy, University of Salerno, Via Giovanni Paolo II, 132, 84084 Fisciano, Italy; midimartino@unisa.it (M.D.M.); piotto@unisa.it (S.P.)
[2] Department of Agriculture, University of Napoli Federico II, Via Università 100, 80055 Portici, Italy; barbara.panunzi@unina.it (B.P.); rosita.diana@unina.it (R.D.)
[3] BIONAM Research Center for Biomaterials, University of Salerno, 84084 Fisciano, Italy
* Correspondence: lucsessa@unisa.it (L.S.); sconcilio@unisa.it (S.C.)

Abstract: Azobenzene photoswitches are fundamental components in contemporary approaches aimed at light-driven control of intelligent materials. Significant endeavors are directed towards enhancing the light-triggered reactivity of azobenzenes for such applications and obtaining water-soluble molecules able to act as crosslinkers in a hydrogel. Here, we report the rational design and the synthesis of azobenzene/alginate photoresponsive hydrogels endowed with fast reversible sol-gel transition. We started with the synthesis of three cationic azobenzenes (AZO A, B, and C) and then incorporated them in sodium alginate (SA) to obtain photoresponsive supramolecular hydrogels (SMHGs). The photoresponsive properties of the azobenzenes were investigated by UV-Vis and ^{1}H NMR spectroscopy. Upon irradiation with 365 nm UV light, the azobenzenes demonstrated efficient *trans*-to-*cis* isomerization, with complete isomerization occurring within seconds. The return to the *trans* form took several hours, with AZO C exhibiting the fastest return, possibly due to higher *trans* isomer stability. In the photoresponsive SMHGs, the minimum gelation concentration (MGC) of azobenzenes was determined for different compositions, indicating that small amounts of azobenzenes could induce gel formation, particularly in 5 wt% SA. Upon exposure to 365 nm UV light, the SMHGs exhibited reversible gel-sol transitions, underscoring their photoresponsive nature. This research offers valuable insights into the synthesis and photoresponsive properties of cationic, water-soluble azobenzenes, as well as their potential application in the development of photoresponsive hydrogels.

Keywords: ionic azobenzenes; photoisomerization; supramolecular hydrogels; sodium alginate; crosslinkers

1. Introduction

Hydrogels are generally hydrophilic systems characterized by highly cross-linked structures associated with ions or cross-linking molecules. In the last decade, their use has increasingly extended into biomedical systems, finding applications in tissue engineering [1], biosensors, and drug delivery vehicles [2].

A hydrogel-based biomaterial may successfully release active compounds such as antibiotics and drugs encapsulated within it. Due to its high-water content, it is like living tissue, has good malleability, and is non-adhesive. Hydrogels can also donate water to a wound site and maintain a wet environment for cell migration, thus promoting faster wound healing [3].

The development of so-called *smart* biomaterials is increasingly the focus of research into new systems that can be variably functionalized to respond to external stimuli (pH, temperature, light,

 doi:10.20944/preprints202403.0536.v1

redox) [4–6]. Light is the most widely used stimulus: safe and non-invasive, it can be easily introduced on demand, and the light source can have a specific wavelength and intensity that can be modulated [7]. Light-responsive biomaterials are commonly prepared by incorporating photoreactive molecules, such as photochromic compounds, into polymer matrices [8–11].

Within the field of photoresponsive molecules, azobenzene has been the most widely used photosensitive component for the design of photoresponsive biomaterials due to an almost degradation-free but mostly reversible isomerization process between the *cis* and *trans* isomers. Photoisomerization of azobenzene can be achieved by selective excitation of the *trans* in the UV range (approx. 365 nm) and the *cis* in the visible range (450 nm) [12,13]. When this molecule is introduced into polymer matrices, the photoisomerization of azobenzene can lead to structural modifications of the material, such as the gel-sol transition of hydrogels [14–17]. Therefore, these materials have been widely used as actuators for the design of optical and electro-optical devices in the biomedical field, as photo-controlled drug delivery, or in tissue engineering [14,18–23].

Recently, more attention has been given to supramolecular hydrogels SMHGs with low molecular weight (LMW) azobenzene as crosslinkers to make photoreactive SMHGs [24–27]. Supramolecular systems offer significant advantages over covalently crosslinked systems because they are more dynamic and formed by interchangeable interactions, such as hydrogen bonds, π-π stacking, and ionic interactions [28–30]. While the use of azobenzene as linkers is commonly reported in the literature for organogel construction [31–33], cases of water-based gels containing azobenzenes are rarer due to their scarce hydrophilicity and adverse synthetic procedure. To facilitate their solubility in water, in some cases, azobenzenes have been modified with peptides [34–36], sugars [37,38], or even azobenzene-based surfactants [16,39,40]. In addition, most of these systems are based on chemical modification of polymers like polyacrylates, polyamides, or alginate with cyclodextrins that, binding with azobenzene, can cause macroscopic changes of polymers physical properties [14,41–44].

In this work, we report the design and synthesis of water-soluble azobenzenes AZO A, AZO B, and AZO C with different ionic head groups. The structural features and photo-isomerization behaviors of these three azobenzenes were studied in detail by UV-vis and ^{1}H NMR spectroscopy. Furthermore, these azobenzenes were successfully used as crosslinkers to build photoresponsive SMHGs by electrostatic interactions with sodium alginate (SA) and π-π stacking interactions between aromatic rings of azobenzene moieties (Figure 1) that stabilized the crosslinked structures of the gels. The hydrogels were characterized by FT-IR spectroscopy and SEM microscopy.

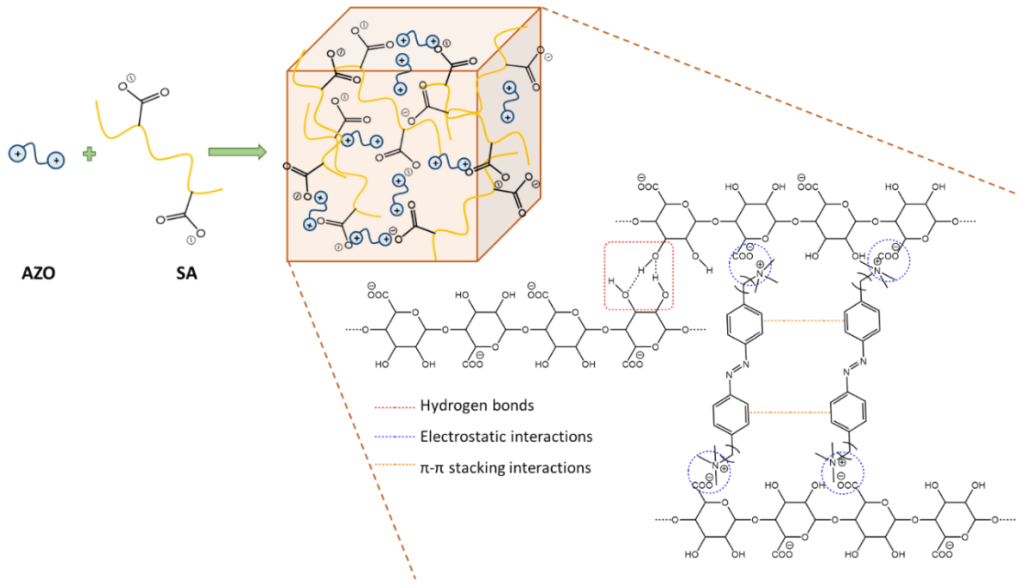

Figure 1. Schematic representation of alginate-azobenzene (AZO A) based supramolecular hydrogels.

 doi:10.20944/preprints202403.0536.v1

2. Materials and Methods

All the reagents and solvents were purchased from Sigma Aldrich (Milan, Italy) and used without further purification.

UV–vis absorption spectra of the samples were recorded at 25 °C at the concentration of 10^{-5} M in MilliQ water on an Evolution 201 spectrophotometer (Thermo Scientific, Rodgau, Germany). The spectral region 600–300 nm was investigated by using a cell path length of 1.0 cm. A UV-vis lamp with a fixed wavelength was used to investigate the isomerization process of azobenzenes in solution and the gel-sol transitions of the hydrogels. The wavelength used for the measurements was 365 ±2 nm with a power of 50 W.

The ^{1}H NMR spectra were recorded with a DRX 400 spectrometer (Bruker, Billerica, MA, USA). The spectra were referenced to residual $CHCl_3$ (^{1}H: δ =7.26 ppm), CH_3OH (^{1}H: δ =3.33 ppm, 4.87 ppm), $(CH_3)_2SO$ (^{1}H: δ =2.50 ppm), or H_2O (^{1}H: δ =4.80 ppm) as indicated. The following abbreviations are used to express spin multiplicities in ^{1}H NMR spectra: s = singlet; d = doublet; dd = double doublet; t = triplet; m = multiplet. For the isomerization study by ^{1}H NMR, the sample was dissolved in deuterium oxide, first kept in the dark, and then irradiated with the UV-vis lamp for 1h and 3h.

High-resolution mass spectra were acquired on an LTQ-Orbitrap instrument (Thermo-Fisher, Waltham, MA, USA) operating in positive ion mode. The molecules were dissolved in methanol or water at a concentration of 0.1 mg/ml and injected into the MS ion source. Spectra were acquired in the 150–900 m/z range.

The infrared spectra were acquired by an FT-IR spectrometer (Spectrum Two FT-IR, Perkin Elmer Massachusetts, USA) at a resolution of 2.0 cm^{-1}, 128 scans, and within a wavelength range of 4000-600 cm^{-1}. The samples were analyzed in powder form; the hydrogels were pre-dried.

SEM analyses were performed using scanning electron microscope, the Leo 1530 Gemini by Zeiss (Carl Zeiss NTS GmbH, Oberkochen, Germany), on the spun films; the operating voltage was 6 kV for all the measurements performed. The hydrogels composed by 5 wt% SA and 1 wt% AZO, were dried before measurement.

2.1. Synthesis of AZO A

All the synthesis patterns and identification numbers of the synthesized molecules can be found in the Supplementary Material, Figures S1 and S2.

Synthesis of 4,4′-(Diazene-1,2-diyl)diphenol (1 in Figure S1)

1.00 g of 4-aminophenol (0.009 mol) was dissolved in an acid solution containing 6.6 ml of distilled water and 1.4 ml of 37% HCl. The suspension was stirred until the reagent was completely solubilized, for approximately 20 minutes, while maintaining a constant temperature in an ice-water bath (0-5°C). Next, 0.695 g $NaNO_2$ (0.010 mol) was dissolved in 1.1 ml of distilled water. The resulting solution was added slowly, drop by drop, to the acid solution containing the aminophenol (Solution A). Meanwhile, a basic solution at pH=14 was prepared by dissolving 0.120 g NaOH in 8.62 ml of distilled water. The resulting basic solution was used to solubilize phenol (0.862 g; 0.009 mol) (Solution B). Solution A was added drop by drop to solution B over a period of half an hour. The reaction mixture was left to stir for about three hours, keeping the temperature (12-15°C) and pH=11 constant. The solution was then neutralized with acetic acid to pH=5-6, resulting in the formation of a precipitate. The precipitate was vacuum filtered, washed with water, and crystallized in EtOH/H_2O. The product obtained was a dark, fine, powdery solid. Yield: 30%. ^{1}H NMR (400 MHz, MeOD): δ 6.97-6.99 ppm (d, 4H), 7.82-7.84 ppm (d, 4H).

Synthesis of 1,2-Bis(4-((6-bromohexyl) oxy)phenyl) Diazene (2 in Figure S1)

0.256 g of compound 1 (0.00119 mol), 0.657 g of K_2CO_3 (0.00476 mol), 1.1 ml of 1,6-dibromohexane (0.00714 mol) were added to 12 ml of acetone in a double-necked flask and left for 24 h at reflux (60°C) under nitrogen atmosphere. The resulting solution was cooled to room temperature, and the solvent was removed by rotavapor. The resulting solid was washed with hexane, followed

 doi:10.20944/preprints202403.0536.v1

by water to remove excess of alkylating agents and salts, and then vacuum filtered. The product obtained was a dark orange solid. Yield: 98%. ^{1}H NMR (400 MHz, $CDCl_3$): δ 1.44-1.47 ppm (m, 8 H), 1.74-1.80 ppm (m, 4H), 1.83-1.88 ppm (m, 4H), 3.35-3.38 ppm (t, 4H), 3.96-3.99 ppm (t, 4H), 6.90-6.93 ppm (d, 4H), 7.78-7.80 ppm (d, 4H).

Synthesis of 6,6'-((Diazene-1,2-diylbis(4,1-phenylene)) bis(oxy))bis(N,N,N-trimethylhexan-1-aminium) (AZO A, Figure S1)

0.300 g of compound 2 was dissolved in trimethylamine solution (18 ml) in a pressure tube. The solution was stirred for 48 hours at 50°C. The resulting mixture was poured into 250 ml diethyl ether, and the precipitate obtained was vacuum filtered and washed several times with diethyl ether to obtain a soluble dark yellow solid. Yield: 97 %. ^{1}H NMR (400 MHz, D_2O): δ 1.34-1.41 ppm (m, 4H), 1.44-1.52 ppm (m, 4H), 1.71-1.81 ppm (m, 8H), 3.03 ppm (s, 18H), 3.24-3.25 ppm (t, 4H), 4.09-4.13 ppm (t, 4H), 7.08-7.10 ppm (d, 4H), 7.76-7.78 ppm (d, 4H). HRMS (ESI+) for $C_{30}H_{50}N_4O_2^{2+}$: m/2z =249.19; found: 249.19.

2.2. Synthesis of AZO B

For the synthesis of compounds 1 and 2 (Figure S1), the same procedure was used as for AZO A.

Synthesis of 1,1'-(((Diazene-1,2-diylbis(4,1-phenylene))bis(oxy))bis(hexane 6,1diyl))bis(pyridin-1-ium) (AZO B, in Figure S1)

50 mg of compound 2 (0.105 mmol) was dissolved in 3 ml of anhydrous CH_3CN, and then 50 µl of pyridine (0.62 mmol) was added. The solution was kept stirring at 70°C for 48h. After the reaction, the solvent was removed by evaporation under reduced pressure. The crude product was washed with ethyl acetate, and the product was obtained as a brown powder with a yield of 68 %. ^{1}H NMR (400 MHz, D_2O): δ 1.31-1.36 ppm (m, 4H), 1.41-1.49 ppm (m, 4H), 1.70-1.76 ppm (m, 4H), 1.94-2.01 ppm (m, 4H), 4.04-4.08 ppm (t, 4H), 4.53-4.56 ppm (t, 4H), 7.03-7.05 ppm (d, 4H), 7.74-7.76 ppm (d, 4H), 7.94-7.97 ppm (t, 4H), 8.38-8.46 ppm (m, 2H), 8.74-8.76 ppm (d, 4H). HRMS (ESI+) for $C_{34}H_{42}N_4O_2^{2+}$ m/2z =269.16; found: 269.16.

2.3. Synthesis of AZO C

Synthesis of N-(4-((4-Hydroxyphenyl)diazenyl)phenyl)acetamide (1′ in Figure S2)

0.400 g of 4-aminoacetalinide (0.0027 mol) was dissolved in an acid solution containing 5.4 ml of distilled water and 570 µL of 37% HCl. The suspension was stirred until the reagent was completely solubilized, for approximately 20 minutes, while maintaining a constant temperature in an ice-water bath (0-5°C). Next, 200 mg $NaNO_2$ was dissolved in 1.2 ml of distilled water. The resulting solution was added slowly, drop by drop, to the acid solution containing the diazonium salt (Solution A). Meanwhile, a basic solution at pH=14 was prepared by dissolving 0.103 g NaOH in 15 ml of distilled water. The resulting basic solution was used to solubilize phenol (0.254 g; 0.003 mol) (Solution B). Solution A was added drop by drop to solution B over a period of half an hour. The reaction mixture was left to stir for about three hours, keeping the temperature (12-15°C) and pH=11 constant. The solution was then neutralized with acetic acid to pH=5-6, resulting in the formation of a precipitate. The precipitate was vacuum-filtered and washed with water. The product obtained was a dark, fine, powdery solid. Yield: 77%. ^{1}H NMR (400 MHz, MeOD): δ 2.18 ppm (d, 3H), 6.91-6.93 ppm (d, 2H), 7.72-7.73 ppm (d, 2H), 7.80-7.85 ppm (q, 4H).

Synthesis of N-(4-((4-(4-Bromobutoxy)phenyl)diazenyl)phenyl)acetamide (2′ in Figure S2)

Compound 1′ (250 mg, 0.98 mmol), 1,4-dibromobutane (1.17 ml, 9.8 mmol), KI (16.3 mg, 0.098 mmol) and K_2CO_3 (271 mg, 1.96 mmol) were dissolved in 10 ml of acetone and the reaction mixture was left to reflux for approximately 4 hours. After this time, the mixture was cooled, and an extraction

 doi:10.20944/preprints202403.0536.v1

was performed to recover the product using a solution of brine and ethyl acetate. The organic phase was recovered and dried, and the solvent evaporated under vacuum. The crude solid was purified by chromatographic column using hexane: ethyl acetate (60:40). The product resulted in a yellow-orange solid, with a yield of 87 %. ^{1}H NMR (400 MHz, MeOD): δ 1.87-1.91 ppm (m, 2H), 1.96-2.01 ppm (m, 2H), 2.06 ppm (s, 3H) 3.43-3.47 ppm (t, 3H), 4.01- 4.04 ppm (t, 3H), 6.95-6.98 ppm (d, 2H), 7.62-7.64 ppm (d, 2H), 7.73-7.78 ppm (q, 4H).

Synthesis of 4-(4-((4-Acetamidophenyl)diazenyl)phenoxy)-N,N,N-trimethylbutan-1-aminium (3′ in Figure S2)

Compound 2′ (200 mg) was dissolved in trimethylamine solution (12 ml) in a pressure tube. The solution was stirred for 48 hours at 50°C. The resulting mixture was added to diethyl ether (250 ml), and the precipitate obtained was vacuum-filtered and washed several times with diethyl ether to obtain a yellow solid. Yield: 92 %. ^{1}H NMR (400 MHz, DMSO): δ 1.78-1.82 ppm (m, 2H), 1.85-1.91 ppm (m, 2H), 2.10 (s, 3H) 3.07 ppm (s, 9H), 3.36-3.40 ppm (t, 2H), 4.13- 4.16 ppm (t, 2H), 7.13-7.15 ppm (d, 2H), 7.78-7.83 ppm (q, 4H), 7.86-7.88 ppm (d, 2H), 10.27 ppm (s, 1H).

Synthesis of 4-(4-((4-Aminophenyl)diazenyl)phenoxy)-N,N,N-trimethylbutan-1-aminium (AZO C)

Compound 3′ (175 mg) was dissolved in 37 % HCl (13 ml) and left stirring overnight at 40°C. The acid was then removed by several additions of distilled water and subsequent evaporation of the solvent, resulting in a dark solid. Yield: 50 %. ^{1}H NMR (400 MHz, DMSO): δ 1.75-1.81 ppm (m, 2H), 1.86-1.92 ppm (m, 2H), 3.08 (s, 9H) 4.10-4.13 ppm (t, 2H), 7.02-7.04 ppm (d, 2H), 7.07-7.09 ppm (d, 2H), 7.62-7.65 ppm (d, 2H), 7.75-7.77 ppm (d, 2H). HRMS (ESI+) for $C_{19}H_{27}N_4O^+$ m/z: 327.22 found: 327.25.

3. Results and Discussion

3.1. Synthesis of Ionic Azobenzenes

The chemical structure of AZO A, AZO B and AZO C are depicted in Figure 2.

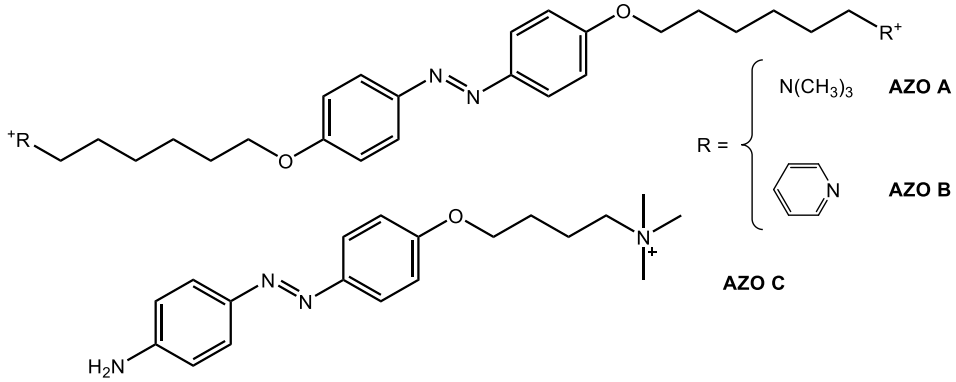

Figure 2. Chemical structure of AZO A, AZO B, and AZO C.

Compounds 1 and 1′ (Figures S1 and S2) were obtained by diazo-coupling reaction [45], forming the diazonium salt in acid media in the presence of sodium nitrite, followed by subsequent reaction with phenol in basic media. For AZO A and B, compound 1 which has two hydroxyl groups in 4,4′ positions on the aromatic rings, is reacted with the alkylating agent 1,6-dibromohexane, and the final products, azobenzenes A and B, gain two charged heads on opposite sides of the azobenzene core [46] by reaction with different amines: AZO A has trimethylammonium heads, AZO B pyridinium heads. In AZO C, compound 1′ has a hydroxyl group and an amide group in the para position, obtained from phenol and amino acetanilide. Compound 2′ (Figure S2) was obtained by the reaction with 1,4-dibromobutane and the introduction of cation head with trimethylamine. Finally, the acid reaction reduced the amide group to amine [47].

 doi:10.20944/preprints202403.0536.v1

The products of all synthetic steps were purified and characterized. ^{1}H NMR spectroscopy and mass spectrometry confirmed the structure of three cationic azobenzenes.

3.2. Light-Responsive Behavior of Azobenzenes

The isomerization study recorded UV-vis absorption and ^{1}H NMR spectra on the synthesized azobenzenes.

For UV-vis analysis, the azobenzenes were dissolved in water at a concentration of 10^{-5}M. Absorption spectra were recorded by keeping the samples in the dark for about 2h to promote complete conversion to the *trans* isomer. Then, the solutions were irradiated by UV light at 365 nm to induce *trans-cis* isomerization. Absorption spectra were recorded at different irradiation times. Maintaining the samples in darkness, relaxation times were measured to assess the time required for the transition back to the *trans* form. For AZO A, complete *trans-cis* isomerization was recorded after 30 seconds of irradiation with UV light at 365 nm (Figure 3a). The spectra show a decrease and shift of the band at about 365 nm related to the $\pi \rightarrow \pi^*$ transition with an increase in the band at 450 nm, relative to the $n \rightarrow \pi^*$ transition. A complete return to *trans* form was achieved in 20 h in the dark (Figure 3b).

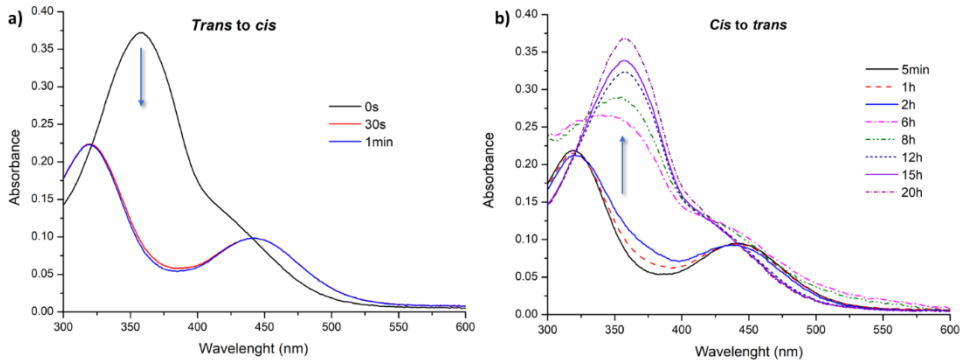

Figure 3. UV-vis spectra of AZO A: (a) *trans* to *cis* isomerization under UV irradiation; (b) *cis* to *trans* relaxation in the dark.

Also for AZO B, *trans-cis* isomerization under UV irradiation at 365 nm was very fast, completed in 1 min (Figure 4a), while the return of the *cis* to the *trans* occurred in 15 hours in the dark (Figure 4b).

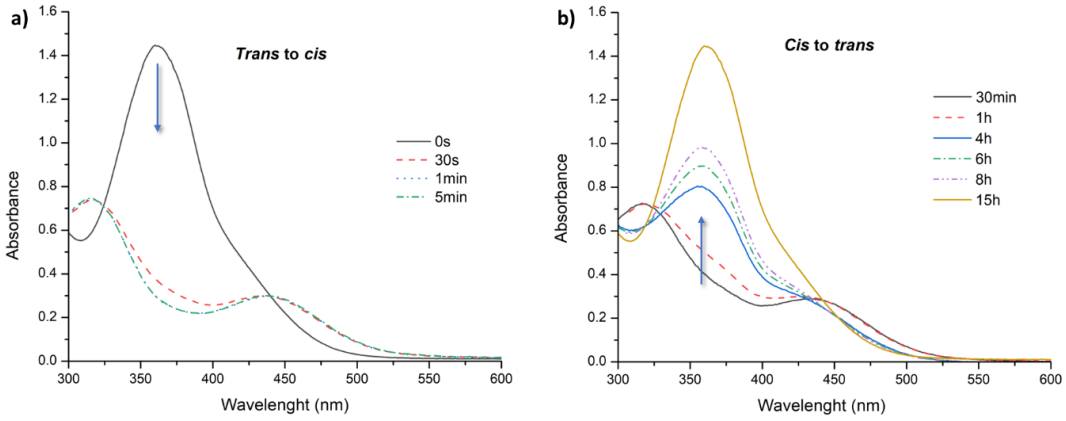

Figure 4. UV-vis spectra of AZO B: (a) *trans* to *cis* isomerization under UV irradiation; (b) *cis* to *trans* relaxation in the dark.

Preprints.org (www.preprints.org) | NOT PEER-REVIEWED | Posted: 8 March 2024 doi:10.20944/preprints202403.0536.v1

The absorption spectrum of AZO C (Figure 5a) showed a shift of about 25-30 nm to longer wavelengths for the band related to the π→ π* transition, leading to overlap between the two transitions, due to the presence of the strong electron-donating amine group in para position [13,48].

The presence of the amine group, similarly, also affected isomerization and relaxation times: the *trans* to *cis* isomerization process for AZO C (Figure 5a) was performed with irradiation at 365 nm in 10 min. The return to the *trans* form (Figure 5b) occurred in about 1h, faster than for the previous azobenzenes, probably due to the higher stability of the *trans* isomer.

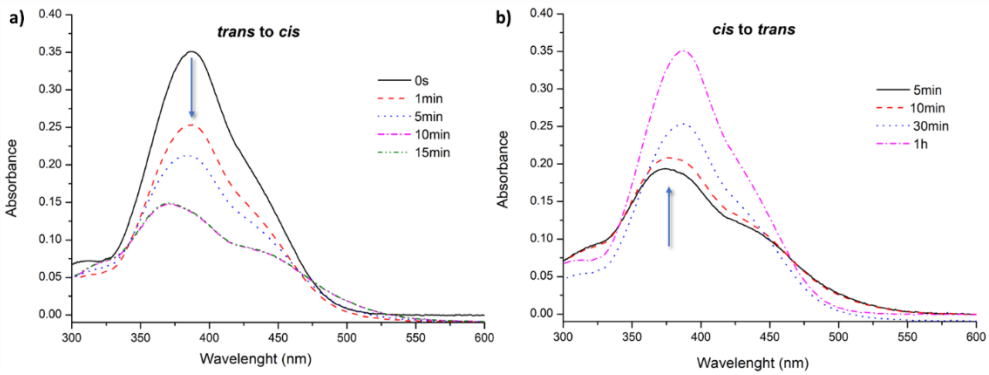

Figure 5. UV-vis spectra of AZO C: (a) *trans* to *cis* isomerization under UV irradiation; (b) *cis* to *trans* relaxation in the dark.

Due to the long relaxation times of AZO A and AZO B, we also studied the photoisomerization process by ^{1}H NMR spectroscopy. As an example, we have reported the ^{1}H NMR isomerization study of AZO A. The sample, solubilized in D_2O, was placed in the dark for 2 h to ensure complete conversion of the molecule to the *trans* isomer (Figure 6, blue line). A first ^{1}H NMR spectrum of the sample irradiated with 365 nm UV light for about 1 h (green line), followed by a second spectrum after 3 h of irradiation (red line), was recorded.

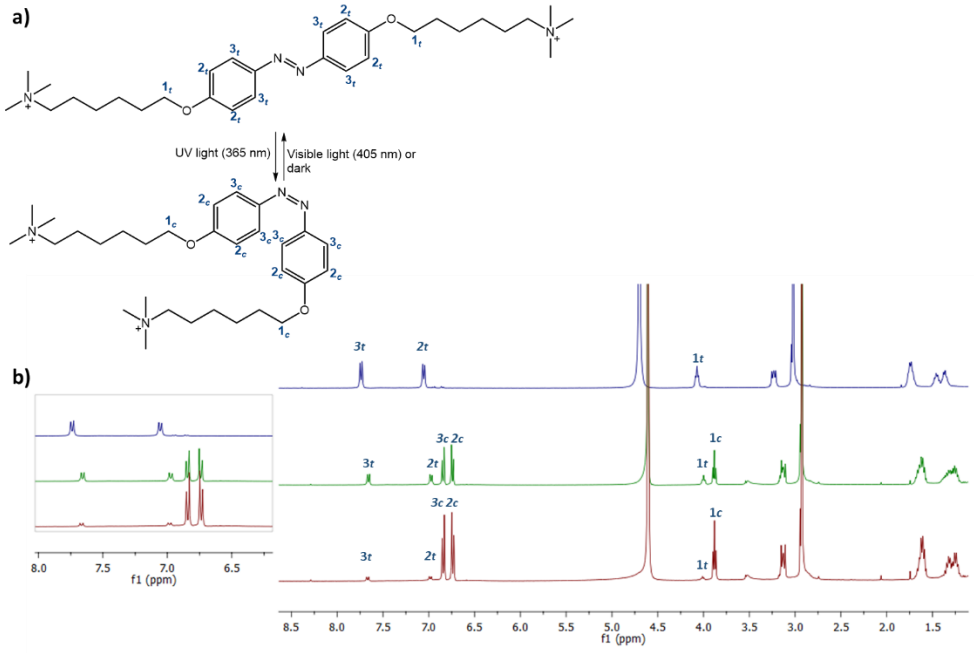

Figure 6. (a) Isomerization process of AZO A; (b) ^{1}H NMR spectra of AZO A after different irradiation times. In the molecules and spectra, the protons of the two *cis* (*c*) and *trans* (*t*) isomers are indicated.

 doi:10.20944/preprints202403.0536.v1

As can be seen in Figure 6, the two isomers exhibit a different proton spectrum, particularly in the aromatic zone (6.5-8.0 ppm) (magnification on the left). The spectrum recorded in the dark shows only the peaks for the *trans* isomer, **1*t***, **2*t*,** and **3*t***. After 1h of UV light irradiation (green line), a new set of proton signals, **1-3*c***, suggested a *trans* to *cis* isomerization. By integrating the proton signals of **2*t***/**2*c*** or **3*t***/**3*c***, the ratio of the two isomers *trans:cis* could be estimated as 49:51. After 3h of UV light irradiation at 365nm (red line), the peaks for the *cis* isomer **1-3*c*** increase, while those for the *trans* isomer decrease, indicating a higher shift in equilibrium towards the *cis* isomer. Integrating the proton signals ratio of the two isomers *trans:cis* could be estimated as 15:85.

3.3. Hydrogels Formation and Photoresponsivity Properties

Alginate is one of the most used natural polymers to form hydrogels characterized by reversible gelation in aqueous solution in the presence of bivalent cations, such as calcium, barium, and magnesium, via ionic crosslinking with carboxyl acid groups of alginate [49]. In this work, the synthesized azo molecules have been used as potential crosslinkers for the development of photoresponsive supramolecular hydrogels SMHGs by electrostatic-type interactions with sodium alginate (SA). We first studied the minimum gelation concentration MGC, which is the minimum concentration of gelator (azobenzene) required to form a stable gel [16], in two different pH conditions: pH=7 and pH=4. The different concentrations of the two components of the hydrogels are shown in Table 1 at pH =7 and Table 2 at pH =4. At pH =4, the amine group in AZO C is protonated, while the carboxyl groups of the alginate remain deprotonated. The pK_a value of alginate carboxyl groups is 3.5 [49,50]. Sodium alginate SA was dissolved in water or an acidic solution at pH= 4, at 60°C. Azobenzene was added while the solution was kept stirring at 60°C. Once the solubilization of azo was complete, the mixture was allowed to cool to room temperature until hydrogel formation (approximately a couple of hours), confirmed by the vial inversion method. Table 1 and Table 2 present the hydrogels' physical states and compositions under two different pH conditions.

Table 1. Hydrogels weight % composition at pH 7.

% wt SA_% wt AZO	8%/0.5%	8%/1%	5%/0.5%	5%/1%
SA_AZO A	V	V	L	L
SA_AZO B	V	V	L	L
SA_AZO C	P	P	P	P

L: liquid; V: viscous; P: precipitate.

Table 2. Hydrogels weight % composition at pH 4.

% wt SA_% wt AZO	8%/0.5%	8%/1%	5%/0.5%	5%/1%	2%/0.5%	2%/1%
SA_AZO A	G (2)	G (4)	L (1)	G (3)	*	*
SA_AZO B	*	*	G (5)	G (6)	L (7)	V (8)
SA_AZO C	*	*	G (9)	G (10)	L (11)	L (12)

L: liquid; V: viscous; G: gel. * No additional tests were carried out beyond the MGC of crosslinking AZO. In brackets are the numbers of the vials, as shown in Figure 7.

As shown in Tables 1 and 2, the three azobenzenes form stable hydrogels with sodium alginate SA under acidic conditions at pH 4. With AZO A, stable hydrogels are formed using 1 wt% (20 mM) of azobenzene with 5 wt% of SA (Figure 7a, vial 3). By increasing the amount of SA to 8 wt%, 0.5 wt% of AZO A (10 mM) is enough to obtain a gel (Figure 7a, vial 2). For AZO B, 0.5 wt% (9 mM) with 5 wt% SA is sufficient for gel formation (Figure 7b, vial 5), probably due to additional π-π interactions between the pyridinium rings. Also, for AZO C, hydrogels were obtained using 0.5 wt% (15 mM) or 1 wt% (30 mM) of azobenzene with 5 wt% of SA (Figure 7c, vials 9 and 10).

Preprints.org (www.preprints.org) | NOT PEER-REVIEWED | Posted: 8 March 2024 doi:10.20944/preprints202403.0536.v1

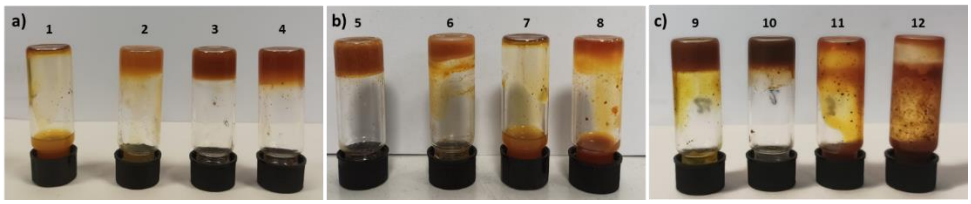

Figure 7. Pictures of hydrogels' physical states at different concentrations of (a) AZO A; (b) AZO B, and (c) AZO C with SA. The numbers on the vials correspond to the concentrations given in Table 2.

To study photoresponsivity, the gels were irradiated with UV light at 365 nm. After a few minutes of irradiation, the hydrogels with AZO A and AZO B showed a transition from gel to sol, following *trans*-to-*cis* isomerization of the azobenzene. For hydrogels with AZO C, an irradiation time of about 30 minutes at 365 nm was required for the gel-sol transition (Figure 8).

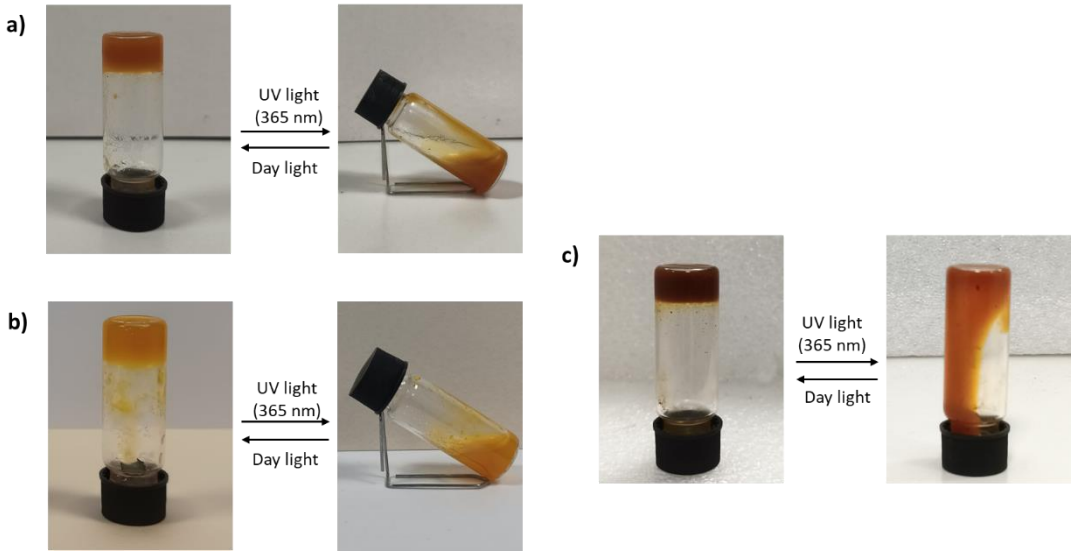

Figure 8. Pictures of hydrogels after UV light and day light irradiation and its gel-sol transition process: (a) 1wt% AZO A + 5wt% SA; (b) 0.5wt% AZO B + 5wt% SA; (c) 0.5wt% AZO C + 5wt% SA.

The *trans* to *cis* azobenzene isomerization causes the SMHGs network to collapse due to the disruption of electrostatic interactions between azobenzenes and SA, transforming SMHGs from gels to solutions. All hydrogels return to the gel state in a few minutes under daylight at room temperature due to the return of azobenzenes to the more stable *trans* form.

3.4. FTIR Characterization of the Hydrogels

The study of the chemical structure of the alginate-azobenzenes hydrogels is critical to investigating the plausible chemical interactions among the compounds. Figure 9 (a, b, and c) shows the IR spectra of SA, AZO A, B, and C as the pure components and the corresponding hydrogels. Pure sodium alginate SA, red curves in spectra a, b, and c of Figure 9, present characteristic absorption bands: around 1600 cm^{-1} and 1412 cm^{-1}, corresponding to the asymmetric and symmetric stretching vibration of the $-COO^-$ groups, respectively; the single bond -CH- vibration band occurs at 2936 cm^{-1} and 1294 cm^{-1}. The intense band from the -C-O-C- stretching occurs around 1024 cm^{-1}, and a large absorption band around 3200 cm^{-1} due to the stretching vibration of the OH group [51]. AZO A spectrum (black curve, Figure 9a) is characterized by symmetric and asymmetric stretching vibration of sp^2 and sp^3 -CH at 3450-3380 cm^{-1} and 2940-2865 cm^{-1}, a series of peaks at 1598-1578 cm^{-1} due to stretching vibration of aromatic rings, the stretching vibration of -N=N- double bond at 1492 cm^{-1}, which is partially overlapped to deformation bands of methylene groups attached to the cationic N^+ at 1475 cm^{-1} [52]. Two strong peaks at 1238 and 1144 cm^{-1} are due to the stretching of -C-N- aromatic

 doi:10.20944/preprints202403.0536.v1

and aliphatic bonds. AZO B spectrum (grey curve in Figure 9b) also shows symmetric and asymmetric stretching vibration of sp^2 and sp^3 -CH in the range between 2800 and 3000 cm^{-1}. In the region of 1600-1400 cm^{-1} there are a series of peaks due to the stretching vibration of aromatic rings of azobenzene nuclei and of pyridinium rings, and at 1242 and 1147 cm^{-1} the stretching of -C-N- aromatic and aliphatic bonds. AZO C spectrum (yellow curve Figure 9c) is characterized by symmetric and asymmetric stretching vibration of -CH and $-NH_2$ group in the region of 3400-2800 cm^{-1}, the last one accompanied by bending vibration peaks at 1650 cm^{-1} and 830 cm^{-1} confirms the presence of a primary amine. Again, there are -N=N- double bond stretching bands at 1547 cm^{-1}, a series of peaks at 1504-1480 cm^{-1} due to benzene rings stretching, and -C-N- (aliphatic and aromatic) bonds at 1379 cm^{-1} and 1253 cm^{-1}. In the spectrum of the SA-AZO A hydrogel (blue curve, Figure 9a), the broadening of the band relative to the OH groups of the alginate is evidence of the formation of hydrogen bonds between polymer chains. The bands corresponding to the $-COO^-$ (1600 cm^{-1} and 1412 cm^{-1}) of SA tend to be less intense, and a slight decrease in the wavenumber due to ionic interaction with azobenzene, as reported in literature for the electrostatic interactions of $-COO^-$ groups of alginate with Ca^{2+} ions [51] and in alginate/chitosan crosslinked hydrogels [53,54]. The same behavior can be observed for the band related to the stretching vibration of the -C-O-C- bonds. The weak peak at 1246 cm^{-1} can be attributed to the stretching vibration of the -CH bond of SA or the band of the -C-N- bond of azobenzene. In both cases, a decrease in intensity and a shift to a lower wave number indicate the presence of interactions between the two components.

In the hydrogel formed by SA with AZO B (purple curve in Figure 9b), as for the hydrogel SA-AZO A, we can see the same shift in the wavenumbers and decrease in intensities of the bands. In the hydrogel formed by SA and AZO C, the azobenzene amine is protonated, and this is confirmed by the presence in the IR spectrum (green curve, Figure 9c) of a band formed by two peaks relating to the vibration stretching of the -N-H bond of the $-NH_3^+$ group at 3300-3190 cm^{-1}, accompanied by bands at 1620 cm^{-1} overlapped with the band relating to the carboxylic group of the alginate and 1400 cm^{-1}.

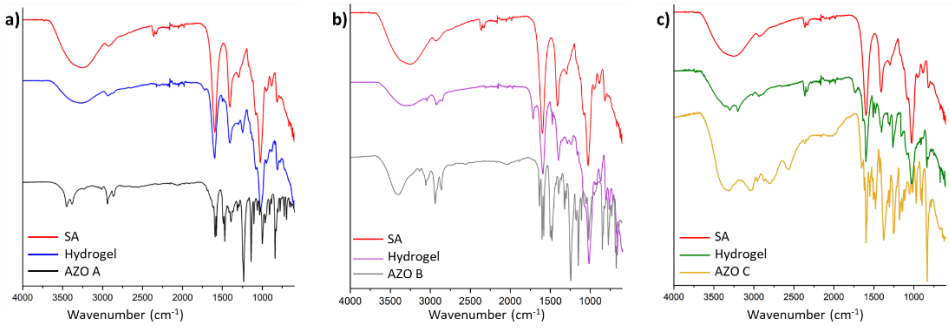

Figure 9. FTIR spectra of the hydrogels (5 wt% SA and 1 wt% AZO) and pure components: (a) AZO A, (b) AZO B and (c) AZO C.

3.5. Hydrogels Morphology

The morphology of the hydrogels was investigated by SEM microscopy. The samples analyzed were composed by 5 wt% SA and 1 wt% AZO.

Figure 10 shows the SEM micrographs of the hydrogel surfaces acquired at different magnifications: 20000 x and 50000 x. The surface of the hydrogels is quite rough, with uneven micropore distribution with irregular shape and size. Specifically, SEM surface images at 50000 x show a higher structuration for the gel with AZO A, which is characterized by clear patterning with rather neat cavities. The structuring is less evident in the case of the sample with AZO B, which shows a rough surface but with fewer evident cavities. Finally, in the case of the gel with AZO C, a flat surface is observed, and no organized cavities are evident. This difference can be ascribed to the different lengths of the three azo-based linkers, two of which (AZO A and B) possess two long tails with terminal charges and one (AZO C), which instead has only one charged tail and an amino group that is not separated from the aromatic system (see Figure 2).

 doi:10.20944/preprints202403.0536.v1

The porous structure offers an advantage for the use of obtained hydrogels as photo-triggered vehicles for the delivery of drugs or biologically active compounds [41,55,56].

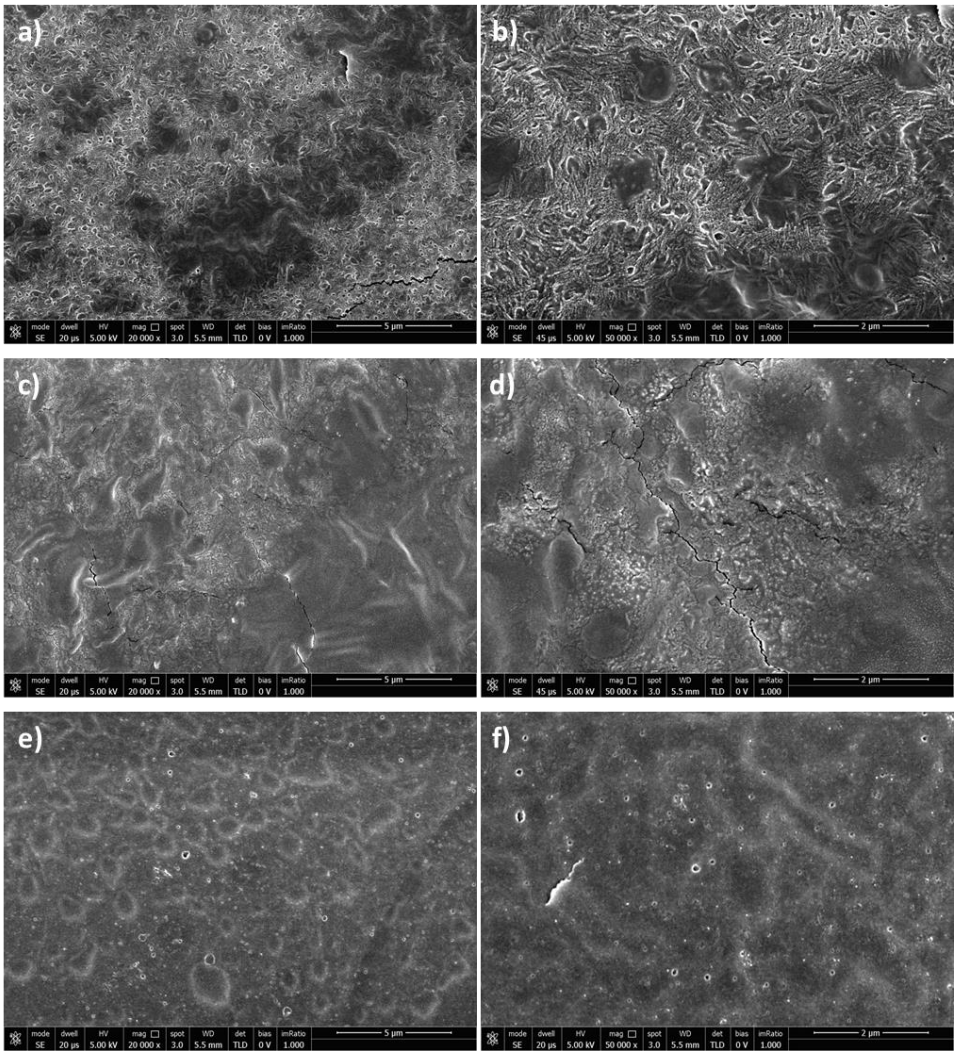

Figure 10. SEM micrographs of the hydrogels surfaces with (a, b) AZO A; (c, d) AZO B; (e, f) AZO C. The magnifications and scale bars are respectively: (a, c, e) 20000 x and 5 μm; (b, d, f) 50000 x and 2 μm.

4. Conclusions

In this study, we have successfully synthesized and characterized photoresponsive supramolecular hydrogels (SMHGs) employing ionic azobenzenes, showcasing their significant potential for applications in smart materials. Incorporating azobenzenes, specifically AZO A, AZO B, and AZO C, into alginate matrices marks a novel approach in creating light-responsive hydrogels. Our findings highlight the control over the hydrogel's synthesis, its reversible and controllable light-responsive behavior, and its morphological characteristics, as underscored by comprehensive FTIR spectroscopy analysis. The tailored photoresponsivity of these compounds under different light stimuli and environmental conditions exemplifies their versatility in modulating the hydrogels' properties, making them promising candidates for developing advanced polymers. These materials exhibit potential applications ranging from drug delivery and tissue engineering to environmental sensing, emphasizing their role in introducing innovative therapeutic delivery methods that respond to external light stimuli.

 doi:10.20944/preprints202403.0536.v1

Future research aim to optimize the photoresponsive efficiency of these hydrogels, explore their biocompatibility for medical applications, and further tailor their physical and chemical properties to enhance performance in specific applications.

Supplementary Materials: The following supporting information can be downloaded at the website of this paper posted on Preprints.org, Figure S1: Synthetic scheme of AZO A and AZO B; Figure S2: Synthetic scheme of AZO C.

Author Contributions: Conceptualization, S.C. and L.S.; investigation, M.D.M. and R.D.; validation, R.D., B.P. and S.P.; formal analysis, S.P.; writing—original draft preparation, M.D.M.; writing—review and editing, S.C.; supervision, B.P.; funding acquisition, S.C. and S.P. All authors have read and agreed to the published version of the manuscript.

Funding: This research was funded by the project NEWROAD, Grant Agreement No 101080024—Cofunded by the European Union, EU4Health Programme (EU4H). L.S. was financed by project PON 2014–2020-Az. IV.4 e IV.6.

Institutional Review Board Statement: Not applicable.

Data Availability Statement: The data presented in this study are contained within the article and Supplementary Materials.

Conflicts of Interest: The authors declare no conflicts of interest.

References

1. Khademhosseini, A.; Langer, R., Microengineered hydrogels for tissue engineering. *Biomaterials* **2007,** 28, (34), 5087-5092.
2. Karimi, S.; Rasuli, H.; Mohammadi, R., Facile preparation of pH-sensitive biocompatible alginate beads havening layered double hydroxide supported metal-organic framework for controlled release from doxorubicin to breast cancer cells. *International Journal of Biological Macromolecules* **2023**, 123538.
3. Zhang, M.; Zhao, X., Alginate hydrogel dressings for advanced wound management. *International Journal of Biological Macromolecules* **2020,** 162, 1414-1428.
4. Mura, S.; Nicolas, J.; Couvreur, P., Stimuli-responsive nanocarriers for drug delivery. *Nature materials* **2013,** 12, (11), 991-1003.
5. Kowalski, P. S.; Bhattacharya, C.; Afewerki, S.; Langer, R., Smart biomaterials: recent advances and future directions. *ACS Biomaterials Science & Engineering* **2018,** 4, (11), 3809-3817.
6. Echeverria, C.; Fernandes, S. N.; Godinho, M. H.; Borges, J. P.; Soares, P. I., Functional stimuli-responsive gels: Hydrogels and microgels. *Gels* **2018,** 4, (2), 54.
7. Di Martino, M.; Sessa, L.; Diana, R.; Piotto, S.; Concilio, S., Recent Progress in Photoresponsive Biomaterials. *Molecules* **2023,** 28, (9), 3712.
8. Dudek, M.; Pokładek, Z.; Deiana, M.; Matczyszyn, K., Molecular design and structural characterization of photoresponsive azobenzene-based polyamide units. *Dyes and Pigments* **2020,** 180, 108501.
9. Sun, S.; Liang, S.; Xu, W.-C.; Xu, G.; Wu, S., Photoresponsive polymers with multi-azobenzene groups. *Polymer Chemistry* **2019,** 10, (32), 4389-4401.
10. Giménez, V. M. M.; Arya, G.; Zucchi, I. A.; Galante, M. J.; Manucha, W., Photo-responsive polymeric nanocarriers for target-specific and controlled drug delivery. *Soft Matter* **2021,** 17, (38), 8577-8584.
11. Li, L.; Scheiger, J. M.; Levkin, P. A., Design and applications of photoresponsive hydrogels. *Advanced Materials* **2019,** 31, (26), 1807333.
12. Jerca, F. A.; Jerca, V. V.; Hoogenboom, R., Advances and opportunities in the exciting world of azobenzenes. *Nature Reviews Chemistry* **2022,** 6, (1), 51-69.
13. Bandara, H. M. D.; Burdette, S. C., Photoisomerization in different classes of azobenzene. *Chemical Society Reviews* **2012,** 41, (5), 1809-1825.

 doi:10.20944/preprints202403.0536.v1

14. Kim, Y.; Jeong, D.; Shinde, V. V.; Hu, Y.; Kim, C.; Jung, S., Azobenzene-grafted carboxymethyl cellulose hydrogels with photo-switchable, reduction-responsive and self-healing properties for a controlled drug release system. *International Journal of Biological Macromolecules* **2020,** 163, 824-832.
15. Rosales, A. M.; Rodell, C. B.; Chen, M. H.; Morrow, M. G.; Anseth, K. S.; Burdick, J. A., Reversible Control of Network Properties in Azobenzene-Containing Hyaluronic Acid-Based Hydrogels. *Bioconjugate Chemistry* **2018,** 29, (4), 905-913.
16. Yang, R.; Peng, S.; Wan, W.; Hughes, T. C., Azobenzene based multistimuli responsive supramolecular hydrogels. *Journal of Materials Chemistry C* **2014,** 2, (43), 9122-9131.
17. Salzano de Luna, M.; Marturano, V.; Manganelli, M.; Santillo, C.; Ambrogi, V.; Filippone, G.; Cerruti, P., Light-responsive and self-healing behavior of azobenzene-based supramolecular hydrogels. *Journal of Colloid and Interface Science* **2020,** 568, 16-24.
18. Karcher, J.; Kirchner, S.; Leistner, A.-L.; Hald, C.; Geng, P.; Bantle, T.; Gödtel, P.; Pfeifer, J.; Pianowski, Z. L., Selective release of a potent anticancer agent from a supramolecular hydrogel using green light. *RSC Advances* **2021,** 11, (15), 8546-8551.
19. Lv, J.-a.; Liu, Y.; Wei, J.; Chen, E.; Qin, L.; Yu, Y., Photocontrol of fluid slugs in liquid crystal polymer microactuators. *Nature* **2016,** 537, (7619), 179-184.
20. Xu, G.; Li, S.; Liu, C.; Wu, S., Photoswitchable Adhesives Using Azobenzene-Containing Materials. *Chemistry–An Asian Journal* **2020,** 15, (5), 547-554.
21. Di Martino, M.; Sessa, L.; Di Matteo, M.; Panunzi, B.; Piotto, S.; Concilio, S., Azobenzene as Antimicrobial Molecules. *Molecules* **2022,** 27, (17), 5643.
22. Peng, K.; Zheng, L.; Zhou, T.; Zhang, C.; Li, H., Light manipulation for fabrication of hydrogels and their biological applications. *Acta Biomaterialia* **2022,** 137, 20-43.
23. Sessa, L.; Concilio, S.; Iannelli, P.; De Santis, F.; Porta, A.; Piotto, S. In *Antimicrobial azobenzene compounds and their potential use in biomaterials*, AIP Conference Proceedings, 2016; AIP Publishing.
24. Wang, T.; Gao, F.; Zhang, Y.; Wang, S.; Li, X.; Zhao, Z.; Dong, Y.; Li, X., Construction of multiresponsive supramacromolecular hydrogels with a novel azobenzene derivative as crosslinkers. *Journal of Materials Research and Technology* **2023,** 22, 1781-1790.
25. Gao, F.; Bi, Z.; Wang, S.; Zhao, Z.; Dong, Y.; Li, X., An amphiphilic azobenzene derivative as a crosslinker in the construction of smart supramacromolecular hydrogels. *Colloids and Surfaces A: Physicochemical and Engineering Aspects* **2022,** 647, 129088.
26. Leistner, A.-L.; Kistner, D. G.; Fengler, C.; Pianowski, Z. L., Reversible photodissipation of composite photochromic azobenzene-alginate supramolecular hydrogels. *RSC Advances* **2022,** 12, (8), 4771-4776.
27. Yang, R.; Jin, W.; Huang, C.; Liu, Y., Azobenzene Based Photo-Responsive Hydrogel: Synthesis, Self-Assembly, and Antimicrobial Activity. *Gels* **2022,** 8, (7), 414.
28. Cheng, Q.; Zhang, Y.; Luan, T.; Wang, Z.; Tang, R.; Xing, P.; Hao, A., Hydrogels Self-Assembled from an Azobenzene Building Block: Stability toward UV Irradiation in the Gel and Thin-Film States. *Chempluschem* **2019,** 84, (4), 328-332.
29. Heeres, A.; van der Pol, C.; Stuart, M.; Friggeri, A.; Feringa, B. L.; van Esch, J., Orthogonal Self-Assembly of Low Molecular Weight Hydrogelators and Surfactants. *Journal of the American Chemical Society* **2003,** 125, (47), 14252-14253.
30. Omar, J.; Ponsford, D.; Dreiss, C. A.; Lee, T. C.; Loh, X. J., Supramolecular hydrogels: Design strategies and contemporary biomedical applications. *Chemistry–An Asian Journal* **2022,** 17, (9), e202200081.

31. Wang, C.; Chen, Q.; Sun, F.; Zhang, D.; Zhang, G.; Huang, Y.; Zhao, R.; Zhu, D., Multistimuli Responsive Organogels Based on a New Gelator Featuring Tetrathiafulvalene and Azobenzene Groups: Reversible Tuning of the Gel−Sol Transition by Redox Reactions and Light Irradiation. *Journal of the American Chemical Society* **2010,** 132, (9), 3092-3096.
32. Balamurugan, S.; Yeap, G.-Y.; Mahmood, W. A. K.; Tan, P.-L.; Cheong, K.-Y., Thermal and photo reversible gel–sol transition of azobenzene based liquid crystalline organogel. *Journal of Photochemistry and Photobiology A: Chemistry* **2014,** 278, 19-24.
33. Lee, S.; Oh, S.; Lee, J.; Malpani, Y.; Jung, Y.-S.; Kang, B.; Lee, J. Y.; Ozasa, K.; Isoshima, T.; Lee, S. Y.; Hara, M.; Hashizume, D.; Kim, J.-M., Stimulus-Responsive Azobenzene Supramolecules: Fibers, Gels, and Hollow Spheres. *Langmuir* **2013,** 29, (19), 5869-5877.
34. Huang, Y.; Qiu, Z.; Xu, Y.; Shi, J.; Lin, H.; Zhang, Y., Supramolecular hydrogels based on short peptides linked with conformational switch. *Organic & Biomolecular Chemistry* **2011,** 9, (7), 2149-2155.
35. Lin, Y.; Qiao, Y.; Tang, P.; Li, Z.; Huang, J., Controllable self-assembled laminated nanoribbons from dipeptide-amphiphile bearing azobenzene moiety. *Soft Matter* **2011,** 7, (6), 2762-2769.
36. Matsuzawa, Y.; Tamaoki, N., Photoisomerization of Azobenzene Units Controls the Reversible Dispersion and Reorganization of Fibrous Self-Assembled Systems. *The Journal of Physical Chemistry B* **2010,** 114, (4), 1586-1590.
37. Ogawa, Y.; Yoshiyama, C.; Kitaoka, T., Helical Assembly of Azobenzene-Conjugated Carbohydrate Hydrogelators with Specific Affinity for Lectins. *Langmuir* **2012,** 28, (9), 4404-4412.
38. Hu, Y.; Zou, W.; Julita, V.; Ramanathan, R.; Tabor, R. F.; Nixon-Luke, R.; Bryant, G.; Bansal, V.; Wilkinson, B. L., Photomodulation of bacterial growth and biofilm formation using carbohydrate-based surfactants. *Chemical science* **2016,** 7, (11), 6628-6634.
39. Peng, S.; Guo, Q.; Hughes, T. C.; Hartley, P. G., Reversible Photorheological Lyotropic Liquid Crystals. *Langmuir* **2014,** 30, (3), 866-872.
40. Yin, C.; Jiang, F.; Li, B.; Wu, L., Multiple modulations for supramolecular hydrogels of bola-form surfactants bearing rigid and flexible groups. *Soft Matter* **2019,** 15, (25), 5034-5041.
41. Chiang, C.-Y.; Chu, C.-C., Synthesis of photoresponsive hybrid alginate hydrogel with photo-controlled release behavior. *Carbohydrate Polymers* **2015,** 119, 18-25.
42. Xie, M.; Wu, C.; Chen, C.; Liu, Y.; Zhao, C., Photo-adaptable shape memory hydrogels based on orthogonal supramolecular interactions. *Polymer Chemistry* **2019,** 10, (35), 4852-4858.
43. He, F.; Wang, L.; Yang, S.; Qin, W.; Feng, Y.; Liu, Y.; Zhou, Y.; Yu, G.; Li, J., Highly stretchable and tough alginate-based cyclodextrin/Azo-polyacrylamide interpenetrating network hydrogel with self-healing properties. *Carbohydrate Polymers* **2021,** 256, 117595.
44. Takashima, Y.; Nakayama, T.; Miyauchi, M.; Kawaguchi, Y.; Yamaguchi, H.; Harada, A., Complex formation and gelation between copolymers containing pendant azobenzene groups and cyclodextrin polymers. *Chemistry letters* **2004,** 33, (7), 890-891.
45. Concilio, S.; Sessa, L.; Petrone, A. M.; Porta, A.; Diana, R.; Iannelli, P.; Piotto, S., Structure Modification of an Active Azo-Compound as a Route to New Antimicrobial Compounds. *Molecules* **2017,** 22, (6), 875.
46. Zinchenko, A. A.; Tanahashi, M.; Murata, S., Photochemical modulation of DNA conformation by organic dications. *ChemBioChem* **2012,** 13, (1), 105-111.
47. Mutter, N. L.; Volarić, J.; Szymanski, W.; Feringa, B. L.; Maglia, G., Reversible Photocontrolled Nanopore Assembly. *Journal of the American Chemical Society* **2019,** 141, (36), 14356-14363.

 doi:10.20944/preprints202403.0536.v1

48. Blevins, A. A.; Blanchard, G. J., Effect of Positional Substitution on the Optical Response of Symmetrically Disubstituted Azobenzene Derivatives. *The Journal of Physical Chemistry B* **2004,** 108, (16), 4962-4968.
49. Maity, C.; Das, N., Alginate-Based Smart Materials and Their Application: Recent Advances and Perspectives. *Topics in Current Chemistry* **2021,** 380, (1), 3.
50. Afzal, S.; Maswal, M.; Dar, A. A., Rheological behavior of pH responsive composite hydrogels of chitosan and alginate: Characterization and its use in encapsulation of citral. *Colloids and Surfaces B: Biointerfaces* **2018,** 169, 99-106.
51. Pereira, R.; Carvalho, A.; Vaz, D. C.; Gil, M. H.; Mendes, A.; Bártolo, P., Development of novel alginate based hydrogel films for wound healing applications. *International Journal of Biological Macromolecules* **2013,** 52, 221-230.
52. Wan, T.; Xu, H.; Yuan, Y.; He, W., Preparation and photochemical behavior of a cationic azobenzene dye-montmorillonite intercalation compound. *Journal of Wuhan University of Technology-Mater. Sci. Ed.* **2007,** 22, 466-469.
53. Baysal, K.; Aroguz, A. Z.; Adiguzel, Z.; Baysal, B. M., Chitosan/alginate crosslinked hydrogels: Preparation, characterization and application for cell growth purposes. *International Journal of Biological Macromolecules* **2013,** 59, 342-348.
54. Li, Z.; Ramay, H. R.; Hauch, K. D.; Xiao, D.; Zhang, M., Chitosan–alginate hybrid scaffolds for bone tissue engineering. *Biomaterials* **2005,** 26, (18), 3919-3928.
55. Xing, Y.; Zeng, B.; Yang, W., Light responsive hydrogels for controlled drug delivery. *Front Bioeng Biotechnol* **2022,** 10, 1075670.
56. Pourbadiei, B.; Adlsadabad, S. Y.; Rahbariasr, N.; Pourjavadi, A., Synthesis and characterization of dual light/temperature-responsive supramolecular injectable hydrogel based on host-guest interaction between azobenzene and starch-grafted β-cyclodextrin: Melanoma therapy with paclitaxel. *Carbohydrate Polymers* **2023,** 313, 120667.